Intramolecular Auger-electron scattering in the ultrafast dissociation of CF4 at the 1s→a1* excitation

著者	Pruemper G., Ueda K., Tamenori Y., Kitajima M., Kuze N., Tanaka H., Makochekanwa C., Hoshino M., Oura M.
journal or publication title	Physical Review. A
volume	71
number	5
page range	052704
year	2005
URL	http://hdl.handle.net/10097/53586

doi: 10.1103/PhysRevA.71.052704

Intramolecular Auger-electron scattering in the ultrafast dissociation of CF_4 at the $1s \rightarrow a_1^*$ excitation

G. Prümper,[1] K. Ueda,[1] Y. Tamenori,[2] M. Kitajima,[3] N. Kuze,[3] H. Tanaka,[3] C. Makochekanwa,[3,4] M. Hoshino,[5] and M. Oura[6]

[1]*Institute of Multidisciplinary Research for Advanced Materials, Tohoku University, Sendai 980-8577, Japan*
[2]*Japan Synchrotron Radiation Research Institute, Sayo-gun, Hyogo 679-5198, Japan*
[3]*Department of Physics, Sophia University, Chiyoda-ku, Tokyo 102-8554, Japan*
[4]*Graduate School of Sciences, Kyushu University, Fukuoka 812-8581, Japan*
[5]*RIKEN, Wako, Saitama 351-0198, Japan*
[6]*RIKEN, SPring-8, Sayo-gun, Hyogo 679-5148, Japan*

(Received 30 December 2004; published 5 May 2005)

We have applied a high-resolution-electron–momentum-resolved-ion coincidence technique to the Auger emission from CF_4 following the F $1s \rightarrow a_1^*$ excitation and found that the Auger electron emitted from the atomic F fragment during the ultrafast dissociation is backscattered by the residual fragment CF_3. We find also that more than half of the excess energy goes into the vibrational excitation of the CF_3 fragment.

DOI: 10.1103/PhysRevA.71.052704 PACS number(s): 34.80.Bm, 32.70.Jz, 32.80.Fb, 33.60.Fy

I. INTRODUCTION

The promotion of a core electron in a molecule into an unoccupied antibonding valencelike orbital causes relaxation of the nuclear frame and electronic shell. In some cases the nuclear relaxation is so rapid that dissociation occurs on the same time scale as Auger-electron emission [1]. The time scale of this competition is of the order of a few femtoseconds and the term "ultrafast dissociation" is often used for describing this femtosecond dissociation. If ultrafast dissociation occurs, atomiclike Auger lines from the atomic fragment and molecular Auger-decay features from the parent molecule coexist in the resonant photoemission spectra. This situation provides a unique opportunity to study details of the femtosecond nuclear dynamics [2–4]. For example, one can measure the speed of the ultrafast dissociation with a "core-hole clock" [5], the interference of the outgoing nuclear wave packets [6], the momentum exchange of the emitted electron with the fast fragment (the emitter) [7–10], etc. Most recently, backscattering of the Auger electron within the dissociating O_2 molecule has been detected [11].

In the present paper, we consider the following sequence of reactions:

$$CF_4 + h\nu \rightarrow CF_4^*(F1s^{-1}a_1^*), \tag{1}$$

$$CF_4^*(F1s^{-1}a_1^*) \rightarrow CF_3 + F^*(1s2p^6\,{}^2S), \tag{2}$$

$$F^*(1s2p^6\,{}^2S) \rightarrow F^+(2p^4\,{}^1D) + e^-. \tag{3}$$

In step (1), a F 1*s* electron in the CF_4 molecule is promoted into the lowest unoccupied antibonding molecular orbital. In step (2), the core-excited molecule dissociates into a core-excited F atom and a CF_3 fragment. We do not analyze the neutral molecular fragments. Thus, in the present work, CF_3 may be considered a symbol summarizing all possible excited or fragmented states involving an C atom and three F atoms. In step (3), the F^* atom emits an Auger electron with a kinetic energy close to 656.5 eV [14]. The lifetime broadening of 0.2 eV corresponds to a lifetime of about 3.3 fs. The Auger electron experiences a shift of its momentum, depending on the emission direction relative to the velocity vector of the emitting F fragment. An energy splitting in the Auger-electron spectrum associated with the different emission directions was first observed for the $1s \rightarrow 3\sigma_u^*$ resonance by Björneholm *et al.* [7] and was termed Doppler shift. A similar energy splitting was observed also in the Auger-electron spectrum of CF_4 corresponding to step (3) [9].

Steps (2) and (3) have no strict order and thus Auger decay can also take place when the core-excited F^* atom may still be close to the CF_3 fragment. Then the electron may be scattered by the CF_3 fragment. So the corresponding angular distribution becomes anisotropic relative to the F-CF_3 dissociation axis. In this situation, one can observe a variation of the shape of the atomiclike Auger line and thus a line-shape analysis gives some insight into the intramolecular scattering process [10]. A more detailed insight into the process is possible in the coincident measurement of the emitted electron with the emitting fragment [11,12]. Performing this type of coincidence experiments, we have successfully obtained evidence that a significant fraction of the Auger electrons emitted from the atomic F fragment undergoes backscattering on the other fragment.

II. EXPERIMENT

The experimental setup and data acquisition system are described elsewhere [12,13] and thus only a brief account is given here. The setup consists of a hemispherical electron spectrometer (Gammadata-Scienta SES-2002) and an ion time-of-flight (TOF) spectrometer mounted inside a vacuum chamber. The sample gas (CF_4 in the present study) is introduced between the pusher and extractor electrodes of the ion spectrometer through a grounded copper needle as an effusive beam. This beam is crossed by the synchrotron radiation. Electrons pass the pusher electrode and enter the electron spectrometer. In order to make coincidence experiments

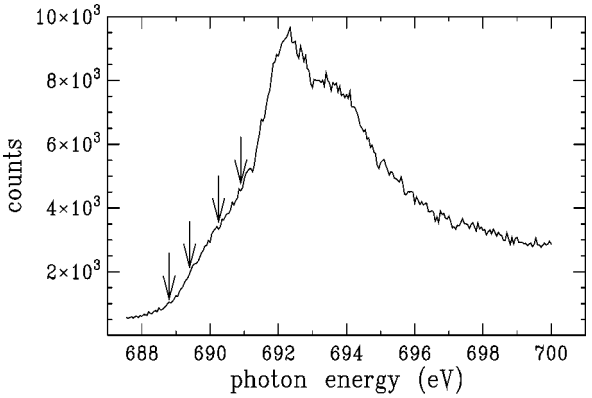

FIG. 1. Total ion yield spectrum of CF_4 in the F 1*s* excitation region. The points marked by arrows indicate four different photon energies at which the coincidence measurements were made.

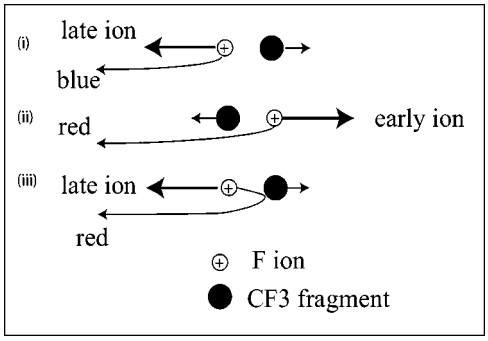

FIG. 2. Schematic diagram of the processes detected in the present coincidence experiment. The direction of the linear polarization of the light is horizontal, leading to fragmentation preferentially in the horizontal direction. Only the electrons ejected in the left direction are detected. Processes (i) and (ii) without scattering can be detected as coincidence events between blueshifted electrons and late ions and between redshifted electrons and early ions, respectively, while process (iii) involving the backscattering can be detected as coincidence events between redshifted electrons and late ions.

possible, a standard charge-coupled-device (CCD) camera of the electron spectrometer was replaced by a delay-line detector (Roentdek DLD40 [15]). During the coincidence experiment, all voltages of the electron spectrometer were fixed. Triggered by the electron detection, rectangular high-voltage pulses with opposite signs are generated by a specially designed pulse generator (GPTA HVC-1000 [16]) and applied to the pusher and extractor electrodes. The ions are detected by another delay-line detector with an active diameter of 80 mm (Roentdek DLD80 [15]) set at the end of the TOF drift tube. All data are recorded in two 8-channel TDC (Roentdeck TDC-8) modules. The data are stored in the list mode for off-line analysis. The contribution from the random coincidences has been subtracted, using the procedure described elsewhere [12].

The experiment has been carried out on the *c* branch of the high-resolution photochemistry beamline 27SU [17–19] at SPring-8, in Japan. The radiation source is a figure-8 undulator [20]. We used first-order harmonic light generated by this undulator which has horizontal linear polarization. We carried out the coincidence experiment at two different resolutions of the electron spectrometer. We used a pass energy of 100 eV and a slit width of 2.5 mm for high-resolution coincidence measurements resolving the Doppler shift of the Auger line and a pass energy of 500 eV and a slit of 4 mm for lower-resolution coincidence measurements. The ionization rate is adjusted by closing the exit slit of the monochromator of the beamline to a level where the rate of random coincidences becomes acceptable [12]. The photon energy bandwidth does not contribute to the observed electron energy width and was estimated as 50 meV. Figure 1 shows the total ion yield spectrum of CF_4 in the F 1*s* excitation region. The points marked by arrows indicate four photon energies 688.80, 689.40, 690.25, and 690.90 eV where the coincidence measurements were made. The photon energy scale was established by setting the peak position of the spectrum in Fig. 1 to 692.25 eV [9].

III. RESULTS AND DISCUSSION

In this work we consider only events where an electron and an F^+ ion are detected in coincidence. Different contributions to the events detected in the coincidence experiment are illustrated in Fig. 2. In order for the electron to be detected, it must be emitted in the direction of the entrance slit of the electron spectrometer, while the F^* atom may fly in any direction. For simplicity, only the F^* atoms flying to the left and right are shown in the figure. These are the most common cases, because the fragmentation preferentially takes place along the linear (horizontal) polarization direction of the light [9]. The processes (i) and (ii) involve only direct emission of the electron without scattering. Thus the "red" and "blue" shifted electrons always correspond to a shorter or larger TOF of the ions, respectively, where the TOF is compared with the TOF of a nonenergetic F^+ ion. The ions are termed "early" and "late" accordingly.

Figure 3 shows an example data set. The correlation of the electron kinetic energy and the component of the ion momentum along the emission direction of the electron (ion TOF) is shown as a coincidence map (c). Each point in the coincidence map corresponds to one electron-ion coincidence event. The corresponding electron kinetic energy spectrum and the ion TOF spectrum are plotted on top (a) and to the right (b), respectively. To guide the eye, the center of the F 1*s* Auger peak in the electron spectrum (a) is marked with a dashed vertical line. Below this peak, two clusters of points marked by the labels (i) and (ii) are visible in the coincidence map (c). They belong to the processes (i) and (ii) in Fig. 2—i.e., coincidence events between blueshifted electrons and late ions and those between redshifted electrons and early ions, respectively.

Knowledge of the fields in the ion spectrometer gives the relation of the TOF and the ion momentum. Knowing the ion momentum from the TOF, the Doppler shift of the electron can be estimated. The gray diagonal line passing through these two clusters of points shows the expected correlation between the ion TOF and the electron kinetic energy. The fact that the events scatter symmetrically around this line indicates that the electron is emitted when the ion has al-

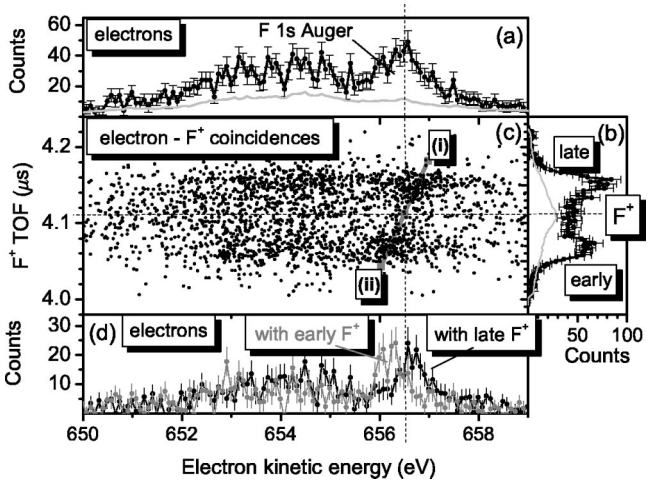

FIG. 3. (a) Electron spectrum coincident with F^+ ions. (b) F^+ ion TOF spectrum coincident with electrons in (a). The black data points in (a) and (b) are all coincident counts. The gray lines below are the random contributions. (c) Coincidence map. Each event is represented by a dot. (d) Electron spectra that are coincident with the "early" and "late" F^+ ions, as illustrated in (b). In this graph the contribution of the random coincidence has been subtracted. The acquisition time for this data set was 24 h.

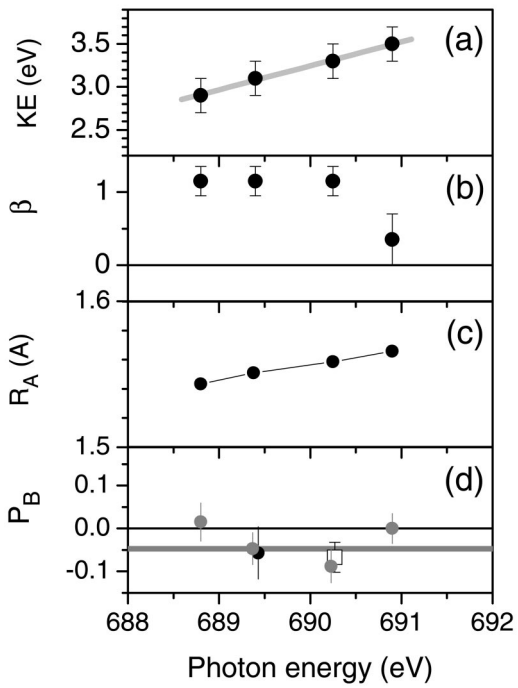

FIG. 4. (a) The kinetic energy of the F^+ fragment determined from the TOF line shape. (b) Asymmetry parameter β of the F^+ fragment. (c) Estimate of the average C—F distance R_A when Auger decay takes place. (d) Early-late asymmetry of the ion TOF peak P_B as a measure of the strength of the backscattering of the Auger electron at the CF_3 remainder. The square data point was measured in an earlier beam time using the same apparatus. The gray line in (d) is the weighted average of all data points.

ready reached its final speed. An earlier emission must lead to a smaller Doppler shift of the electron. Thus we can conclude that Auger decay takes place in the atomic regime. In this sense, we have direct proof that the first phase of the fragmentation, the acceleration of the core-excited F^* atom, is faster than the Auger decay.

An alternative way to illustrate the momentum correlation of the electron and ion is given by graph (d). To create the two electron spectra the coincidence map has been cut into two parts. The horizontal dashed line around 4.1 μs marks the TOF of F^+ ions with zero momentum along the spectrometer axis. From the contributions of the coincidence events above and below this line, the two electron spectra in graph (d) have been calculated. In this figure the Doppler shift of the F 1*s* Auger line is clearly visible, even though no Doppler splitting is resolved in graph (a).

The line shape of the F^+ ion TOF spectrum in Fig. 3(c) reflects the distribution of one component of the ions momentum. Therefore, assuming a single fragmentation energy and an angular distribution described by an anisotropy parameter β, a line-shape analysis can yield values for the kinetic energy and β. In order to extract energies and anisotropies of the F^+ ions, we have performed a Monte Carlo simulation of the time of flight of about 10^6 ions produced in an extended source volume with a given energy and angular anisotropy. Knowing all the dimensions of the spectrometer, the trajectories of the ions were calculated, assuming static homogeneous electric fields. Great care was taken in the mechanical design of the ion time-of-flight spectrometer and the high-voltage pulse generator to justify this assumption. The details of the procedure are described elsewhere [12]. Here we give only a brief qualitative description. The kinetic energy and anisotropy are determined from a comparison of the observed and calculated peak shapes. The overall width of the profile reflects the fragmentation energy while the dip in the center of the profile reflects the anisotropy.

In order to determine the F^+ kinetic energy, it is sufficient to resolve the early and late ions. The energy resolution of the electron spectrometer is only necessary to restrict the set of coincidence events to the Auger line. In order to study the F^+ kinetic energy dependence on the excitation energy, measurements were performed at the four photon energies marked in the total ion yield spectrum in Fig. 1. With a pass energy of 500 eV and a slit width of 4 mm the data acquisition time could be reduced to 6 h for each data point. The results for the kinetic energy and the anisotropy are plotted as a function of photon energy in Figs. 4(a) and 4(b), respectively. Only ions coincident with the Auger line were used for this evaluation. The β value stays constant ($\beta \simeq 1.2$) for 688.80–690.25 eV. It decreases to 0.4 at an energy 690.90 eV, implying that the resonance is not isolated anymore and starts to overlap with another electronic state.

If all of the excess energy was given to the F^+ ion, we would observe a slope of 1 in graph (a) of Fig. 4. If a rigid CF_3 fragment is assumed, one would expect a slope of $69/(69+19)=0.784$, as the energy-sharing ratio is determined by the mass ratio 19:69 for the fragments F^+ and CF_3 due to momentum conservation. If the central C atom can be moved freely, the recoil of the F atom is received only by the C atom. Then the dissociation leads to less energetic F^+ ions because of an energy sharing of 19:12 for C and F. This

results in a slope of $12/(19+12)=0.387$. The observed average slope is only 0.275, suggesting that the F^+ ion receives even less energy. A model taking into account the configuration relaxation of CF_3 is needed to understand this energy sharing. Let us consider the ground-state configurations: CF_4 is tetrahedral with F—C—F angle of 109.5°. If one F atom is removed, the CF_3 ground state becomes trigonometric pyramidal with F—C—F angle of 111.3° [21]. Thus, when the F atom departs from the CF_4 molecule, the C atom is pulled back by the three remaining F atoms. This may explain that the energy release is less than the expectations described above.

Because of momentum conservation, the kinetic energy sharing between F^+ and CF_3 is 69:19. The total kinetic energy release is therefore 1.275 times the F^+ kinetic energy. Thus $0.275\times1.275=0.355$ of the excess energy goes to the F-CF_3 fragmentation and 0.645 goes to the vibrations and/or further fragmentations of CF_3.

Using the observed kinetic energy of the F^+ ion and momentum conservation, we can calculate the asymptotic speed at which the F^+ moves away from the center of mass of CF_3. For this estimate, we assume a rapid acceleration to the asymptotic speed. Thus the C—F distance R_A at the Auger decay is given by the ground-state distance of $r_0=1.315$ Å and the speed times the Auger lifetime [10]. The result of this is shown in Fig. 4(c). Because of the short Auger lifetime, this distance is still close to r_0.

If a significant fraction of the electrons that are emitted in the direction of CF_3 undergo scattering, this will lead to a reduction of the count rate for process (ii) because the electron is no longer detected and, instead, process (iii) in Fig. 2 may be detected for electrons that are initially emitted away from the electron detector and then reflected in its direction. Process (iii) can be distinguished from (i) and (ii) as a coincidence signal between the redshifted electron and the late ion. The degree of the early-late asymmetry (the probability of the backscattering) can be defined as

$$P_B=\frac{I_\mathrm{l}-I_\mathrm{e}}{I_\mathrm{l}+I_\mathrm{e}}, \tag{4}$$

where I_l and I_e are the integrated intensity (area) of the late and early ions, detected in coincidence with an Auger electron, as illustrated in Fig. 3(b). The results for the early-late asymmetry are shown in Fig. 4(d). The backscattering is found to be significant: it has an average value of $P_B=4.7\%$ of the total coincident intensity. In such a situation interference effects in the electron spectra due to the two indistinguishable paths [22]—direct emission and reflection—at the remainder may occur, for the fragmentation perpendicular to the electron spectrometer where the Doppler shift is negligible. However, the statistics in this experiment do not allow such a discussion.

In conclusion, we have performed an electron-momentum-resolved ion coincidence measurement for Auger-electron emission from CF_4 following F $1s\rightarrow a_1^*$ excitation. We found that more than half of the excess energy is absorbed by the internal degrees of freedom of the CF_3 remainder. We found that about 5% of the Auger electrons emitted by the atomic F fragment during the ultrafast dissociation along the electric vector of the light are backscattered by the residual fragment CF_3.

ACKNOWLEDGMENTS

The experiment was carried out with the approval of the SPring-8 program review committee and was partly supported by the Japan Society of the Promotion of Science (JSPS) in the form of Grants-in-Aid for Scientific Research. The staff of Spring-8 are greatly acknowledged for providing an excellent experimental facility.

[1] P. Morin and I. Nenner, Phys. Rev. Lett. **56**, 1913 (1986).
[2] F. Gel'mukhanov and H. Ågren, Phys. Rev. A **54**, 379 (1996).
[3] E. Pahl, L. S. Cederbaum, H.-D. Meyer, and F. Tarantelli, Phys. Rev. Lett. **80**, 1865 (1998).
[4] F. Gelmukhanov, V. Kimberg, and H. Ågren, Phys. Rev. A **69**, 020501(R) (2004).
[5] O. Björneholm, S. Sundin, S. Svensson, R. R. T. Marinho, A. Naves de Brito, F. Gel'mukhanov, and H. Ågren, Phys. Rev. Lett. **79**, 3150 (1997).
[6] R. Feifel *et al.*, Phys. Rev. Lett. **85**, 3133 (2000).
[7] O. Björneholm, M. Bässler, A. Ausmees, I. Hjelte, R. Feifel, H. Wang, C. Miron, M. N. Piancastelli, S. Svensson, S. L. Sorensen, F. Gel'mukhanov, and H. Ågren, Phys. Rev. Lett. **84**, 2826 (2000).
[8] A. Baev, F. Gel'mukhanov, P. Sałek, H. Ågren, K. Ueda, A. de Fanis, K. Okada, and S. Sorensen, Phys. Rev. A **66**, 022509 (2002).
[9] K. Ueda, M. Kitajima, A. De Fanis, T. Furuta, H. Shindo, H. Tanaka, K. Okada, R. Feifel, S. L. Sorensen, H. Yoshida, and Y. Senba, Phys. Rev. Lett. **90**, 233006 (2003).
[10] M. Kitajima, K. Ueda, A. De Fanis, T. Furuta, H. Shindo, H. Tanaka, K. Okada, R. Feifel, S. L. Sorensen, F. Gel'mukhanov, A. Baev, and H. Ågren, Phys. Rev. Lett. **91**, 213003 (2003).
[11] O. Kugeler, G. Prümper, R. Hentges, J. Viefhaus, D. Rolles, U. Becker, S. Marburger, and U. Hergenhahn, Phys. Rev. Lett. **93**, 033002 (2004).
[12] G. Prümper, Y. Tamenori, A. De Fanis, U. Hergenhahn, M. Kitajima, M. Hoshino, H. Tanaka, and K. Ueda, J. Phys. B **38**, 1 (2005).
[13] G. Prümper, K. Ueda, U. Hergenhahn, A. De Fanis, Y. Tamenori, M. Kitajima, M. Hoshino, and H. Tanaka, J. Electron Spectrosc. Relat. Phenom. (to be published).
[14] S. Svensson, L. Carlsson, N. Mårtensson, P. Baltzer, and B. Wannberg, J. Electron Spectrosc. Relat. Phenom. **50**, C1 (1990).
[15] See http://roentdek.com for details on the detectors.
[16] See http://www.gpta.de for details on the HV pulse generator.
[17] H. Ohashi, E. Ishiguro, Y. Tamenori, H. Kishimoto, M. Tanaka, M. Irie, T. Tanaka, and T. Ishikawa, Nucl. Instrum. Methods Phys. Res. A **467–468**, 529 (2001).

[18] H. Ohashi, E. Ishiguro, Y. Tamenori, H. Okumura, A. Hiraya, H. Yoshida, Y. Senba, K. Okada, N. Saito, I. H. Suzuki, K. Ueda, T. Ibuki, S. Nagaoka, I. Koyano, and T. Ishikawa, Nucl. Instrum. Methods Phys. Res. A **467–468**, 533 (2001).
[19] Y. Tamenori, H. Ohashi, E. Ishiguro, and T. Ishikawa, Rev. Sci. Instrum. **73**, 1588 (2002).
[20] T. Tanaka and H. Kitamura, J. Synchrotron Radiat. **3**, 47 (1996).
[21] M. Simon, P. Morin, P. Lablanquie, M. Lavollée, K. Ueda, and N. Kosugi, Chem. Phys. Lett. **238**, 42 (1995).
[22] N. Stolterfoht, B. Sulik, V. Hoffmann, B. Skogvall, J. Y. Chesnel, J. Rangama, F. Frémont, D. Hennecart, A. Cassimi, X. Husson, A. L. Landers, J. A. Tanis, M. E. Galassi, and R. D. Rivarola, Phys. Rev. Lett. **87**, 023201 (2001).